Disentangling the Components of the Milky Way

Inferring the Structure of the Milky Way in Phase-Space Using Gaussian Mixture Modelling with Extreme Deconvolution

A REPORT PRESENTED

BY

RAUNAQ RAI

Departments

Department of Physics (Cavendish Laboratory)
Institute of Astronomy

Degree

MPhil in Data Intensive Science

Supervision

Dr Anke Arentsen

St Edmund's College
University of Cambridge

29th June 2025

Abstract

Contents

List of Figures

List of Tables

1 Introduction

The Milky Way Galaxy, host to our solar system, is a spiral galaxy with a centre located approximately 150 000 trillion miles (or 25 000 lightyears) from Earth. Its formation history is complex and remains an active area of research. Being embedded within the Milky Way means we can study it in greate detail than any external galaxy, testing models of galaxy formation with high-precision observational data. One of the central aims of Galactic Archaeology is to reconstruct the Milky Way's assembly by examining the chemical compositions and dynamical properties of its stars.

In this project, we replicate and extend the analysis of Zhang et al. [2024], who investigated a very metal-poor disc component in the Milky Way. Very metal poor stars, formed from an interstellar medium unpolluted by earlier generations of supernovae, are among the oldest relics in the Galaxy. Discovering them on disc-like orbits would challenge the conventional view that the disc formed later from already enriched gas [Bland-Hawthorn and Gerhard, 2016], implying instead an earlier onset of disc assembly. Using Gaia DR3, the original study applied a Gaussian Mixture Model with Extreme Deconvolution to the velocity distributions of stars across metallicity bins, probing whether a coherent disc signal persists down to the lowest metallicities.

1.1 Components of the Milky Way

The Milky Way is commonly decomposed into four stellar components: a *thin disc*, a *thick disc*, a central *bulge/bar*, and a roughly spherical *halo* [Bland-Hawthorn and Gerhard, 2016, Helmi, 2020]. The thin disc dominates, containing $\sim 90\%$ of all stars and most of the interstellar gas. Ongoing star formation is concentrated in the "molecular–gas ring" at Galactocentric radii $R \simeq 4$–8 kpc, where young ($\lesssim 1$ Gyr), metal-rich stars trace nearly circular, co-rotating orbits with low velocity dispersion ($\sigma_\phi \simeq 20\ \mathrm{km\,s^{-1}}$). Above the mid-plane lies the thick disc: an older ($\gtrsim 8$–10 Gyr), moderately metal-poor population with [Fe/H] ~ -0.6 to -1.0, a scale height of $z_{\mathrm{scale}} \approx 1$ kpc, and hotter kinematics ($\sigma_z \simeq 40\ \mathrm{km\,s^{-1}}$) while still retaining net prograde rotation. Inside $R \lesssim 2$ kpc, the central bulge—partly bar-shaped—hosts both old, metal-rich stars and a younger, actively forming component; stellar motions there combine bar-driven streaming with high random velocities ($\sigma \sim 100\ \mathrm{km\,s^{-1}}$). Encasing all of these is the stellar halo, which contributes only a few per cent of the total stellar mass yet harbours the Galaxy's oldest, most metal-poor stars ([Fe/H] $\lesssim -1.5$) on highly eccentric or even retrograde orbits. Its low density, rich substructure, and extreme kinematics reveal an origin in the hierarchical accretion and tidal disruption of dwarf galaxies and globular clusters. Together, the spatial distribution, chemistry, and dynamics of these four components encode the Milky Way's star-formation history and its sequence of merger events.

1.2 Metallicity as a Cosmic Clock

Precise ages for individual old stars are notoriously difficult to measure, so their chemical composition - most commonly the iron-to-hydrogen ratio, [Fe/H] - is often used as a surrogate clock. Very metal-poor (VMP) stars must have formed before successive generations of Type II and Type Ia supernovae had substantially enriched the interstellar medium, and therefore exhibit low [Fe/H] values. Metallicity is inferred spectroscopically from the equivalent widths of metal absorption lines such as Fe I and the Ca II K line; after

correcting for effective temperature and surface gravity, their relative strengths give elemental abundances. Large surveys (for example APOGEE, GALAH, LAMOST, and the Gaia XP spectra) now provide such measurements for millions of stars, enabling empirical age–metallicity relations that link chemistry to stellar chronometry [e.g. Nordström et al., 2004, Haywood et al., 2013, Leung and Bovy, 2019, Anders et al., 2023]. These studies consistently show that stars with [Fe/H] $\lesssim -1$ are typically older than $\sim 10\,\mathrm{Gyr}$, making low-metallicity populations valuable probes of the Milky Way's earliest disc-building epochs.

1.3 ΛCDM : hierarchical growth and a lopsided halo

In the concordance ΛCDM model, galaxy-sized haloes assemble *hierarchically*: small dark-matter clumps form first and then merge to build larger structures. Cosmological N-body simulations demonstrate that the number of subhaloes of mass M obeys $\mathrm{d}n/\mathrm{d}M \propto M^{-1.9}$, a near power-law over many decades in mass [Cooper et al., 2010, Fall and Chandar, 2012]. For a Milky-Way–sized halo this translates to

- $\sim 10^2$ **minor** accretions with $M_{\mathrm{sub}} \lesssim 10^9\,M_\odot$, and
- a few **major** events with $M_{\mathrm{sub}} \gtrsim 10^{10}\,M_\odot$

over a Hubble time.

Only a small subset of these haloes ever form appreciable numbers of stars. Below a critical virial mass $M_{\mathrm{vir}} \sim 10^{11}\,M_\odot$, re-ionisation and stellar feedback drastically reduce the efficiency of turning gas into stars. Consequently, the stellar-mass–halo-mass (SMHM) relation becomes very steep at the low-mass end [Purcell et al., 2007, Bullock and Boylan-Kolchin, 2017]: most low-mass subhaloes are effectively "dark", whereas a few relatively massive dwarfs are luminous.

Hence, while the Milky Way has absorbed *hundreds* of subhaloes, **one or two** of the most massive dwarfs contribute the majority of the halo's stellar mass; the rest add little more than dark matter and dynamical substructure.

Once accreted, dynamical friction drags the most massive satellites deep into the Galactic potential, their orbits radialise, and their debris is dispersed throughout the *inner* halo. The disrupted stars inherit coherent signatures—high radial anisotropy, distinctive angular momenta, and chemically narrow sequences—that survive to the present [e.g. Helmi and Tim de Zeeuw, 2000]. Consequently, the stellar halo is not a smooth spheroid but a map of the Galaxy's merger history, with the inner halo overwhelmingly shaped by a few dominant progenitors (e.g. Gaia–Sausage/Enceladus), and the outer halo supplied by many low-mass accretions.

1.4 Accretion versus *in-situ* disc formation

Chemical and kinematic evidence confirms that the metal-poor halo is primarily accreted. The debris of the Gaia–Sausage/Enceladus (GSE) event, for instance, is traced by stars with $-2 < [\mathrm{Fe/H}] < -1$ and extreme orbital anisotropy ($\beta \gtrsim 0.8$; Belokurov et al. 2018, Helmi et al. 2018). At [Fe/H] $\lesssim -2$ an even broader mix of minor mergers emerges, erasing any global rotation signal [Lancaster et al., 2019, Bird et al., 2021].

Against this backdrop, a number of studies have uncovered stars in the range $-2 < [\mathrm{Fe/H}] < -1$ whose velocities resemble a *disc*: modest eccentricities and net prograde rotation [Norris et al., 1985, Chiba and Beers, 2000, Carollo et al., 2019, An and Beers, 2020]. Gaia has pushed this frontier to $[\mathrm{Fe/H}] < -2$ [Sestito et al., 2019, Venn et al., 2020, Cordoni et al., 2020, Mardini et al., 2022]. Whether these objects represent (i) an *in-situ* metal-poor disc or (ii) the spun-up debris of earlier mergers remains hotly debated.

1.5 Origins of very-metal-poor disc candidates

Three broad formation scenarios have been proposed:

1. **Early *in-situ* disc.** Stars form in a gas-rich disc before $z \sim 4$, and later migrate outward or are dynamically heated; such stars would share the chemistry of the proto-Galaxy.
2. **Proto-galactic building blocks.** VMP stars originate in several massive, gas-rich satellites accreted at high redshift; their debris is dragged into the disc plane as the gaseous disc settles [e.g. Sestito et al., 2020].
3. **Late, minor prograde mergers.** Low-mass satellites on aligned orbits are assimilated after the disc forms, depositing a thin layer of metal-poor stars that retain disc-like kinematics [Santistevan et al., 2021].

Cosmological simulations generally reproduce scenario 2, finding that early mergers dominate the VMP budget while a coherent disc does not appear until $z \lesssim 2$ [Gurvich et al., 2023].

Observationally, Belokurov and Kravtsov [2022] identified *Aurora*, a kinematically hot, weakly rotating population with $-2 \lesssim [\mathrm{Fe/H}] \lesssim -1.3$, arguing against an extremely early disc. Follow-up work shows Aurora to be centrally concentrated [Rix et al., 2022, Arentsen et al., 2020a,b], consistent with heated debris rather than a long-lived thin disc. Furthermore, secular processes such as bar–halo resonances can impart a modest prograde bias to halo stars, mimicking a disc signal [Dillamore et al., 2023].

Unravelling these possibilities demands six-dimensional phase-space information and precision abundances— the focus of the present study.

1.6 This Work

In this study we assess the claim that the Milky Way hosts a *very-metal-poor* (VMP; $[\mathrm{Fe/H}] < -2$) stellar disc. Our data set is drawn from *Gaia* DR3, which supplies six–dimensional phase–space coordinates—sky position, parallax–based distance, proper motions, and radial velocity—for each star, together with homogeneous metallicity and α-element abundances from the *Gaia* XP pipeline. To disentangle kinematic sub-populations we model, in successive narrow metallicity bins, the full three-dimensional velocity distribution (v_R, v_ϕ, v_z) with a Gaussian Mixture Model whose parameters are inferred via *Extreme Deconvolution*; the XD formalism explicitly folds the individual distance and proper-motion uncertainties into the likelihood, ensuring that measurement noise does not bias the recovered velocity moments.

Astrophysically, a genuine disc should manifest itself as a high-weight Gaussian centred near the Local Standard of Rest ($v_\phi \simeq 220\ \mathrm{km\,s^{-1}}$) with small tangential and vertical

dispersions ($\sigma_\phi, \sigma_z \lesssim 30$ km s^{-1}) and negligible mean radial motion, whereas the halo or any heated component should appear as a broad, almost isotropic Gaussian with little net rotation and dispersions of order 120–150 km s^{-1}. By tracking how the weight of the cold, rotating component varies with metallicity we can determine when ordered rotation first emerged and test whether VMP stars were formed in situ or accreted from a satellite.

2 Data

2.1 Sample construction

Our parent catalogue is the bright ($G < 16$) red–giant–branch sample of Andrae et al. [2023]. Stellar metallicities are predicted with an eXtreme-Gradient-Boosting (XGBoost[1]) model trained on high-resolution APOGEE DR17 spectra and a supplementary set of very metal-poor stars, ensuring reliable performance down to [M/H] $\simeq -3.5$. For each of the 17.6 million giants the catalogue delivers homogeneous values of [M/H], $T_{\rm eff}$, and $\log g$ with a quoted random uncertainty of $\simeq 0.1$ dex in [M/H] at $G \lesssim 15$. We retain only entries flagged as "high-confidence" and lying in $-3.5 <$ [M/H] $< +0.5$.

Astrometric positions, proper motions, and radial velocities come from the main *Gaia* DR3 tables [Gaia Collaboration et al., 2023], while heliocentric distances are adopted from the Bayesian photo-geometric catalogue of Bailer-Jones et al. [2021]. Because accurate velocities scale with distance precision, we impose a fractional-parallax-uncertainty cut $\sigma_\varpi/\varpi < 0.10$ (FPU); stars that fail this threshold are discarded.

XP spectra are susceptible to reddening: heavy extinction dims the sources, lowers the XP signal-to-noise ratio, and biases the machine-learning metallicities. To minimise such systematics we exclude stars with $E(B-V)_{\rm SFD} > 0.5$ or Galactic latitude $|b| < 10°$, using colour-excess values from the SFD map accessed via DUSTMAPS [Green, 2018]. These criteria remove regions where dust corrections are large and spatially variable, at the expense of a modest loss of sky coverage.

Field-star kinematics can also be skewed by dense sub-structures. Accordingly we mask all objects lying within 1° of any known globular cluster or dwarf-galaxy satellite, following the list compiled by Pace [2024]. This step eliminates obvious non-field populations (e.g. cluster members and recent accretion debris) without significantly reducing the statistical power of the sample.

After the metallicity flag, distance–quality, reddening, latitude, and sub-structure cuts, our working data set comprises $\sim 3.4 \times 10^6$ red-giant stars possessing homogeneous metallicities and full six-dimensional phase-space information. This curated sample underpins the chemo-kinematic analysis presented in the remainder of this report.

2.2 Galactocentric Positions and Velocities

Six–dimensional phase–space coordinates are obtained with `astropy.coordinates`. We adopt a Galactocentric frame with $R_0 = 8.1$ kpc and $Z_0 = 25$ pc [McMillan, 2016], and a solar velocity[2] $(U_\odot, V_\odot, W_\odot) = (11.1, 245, 7.25)$ km s^{-1} [Schönrich et al., 2010]. The

[1] eXtreme Gradient Boosting

[2] Cartesian components (U, V, W), where U is radially outwards, V is aligned with Galactic rotation, and W points to the North Galactic Pole.

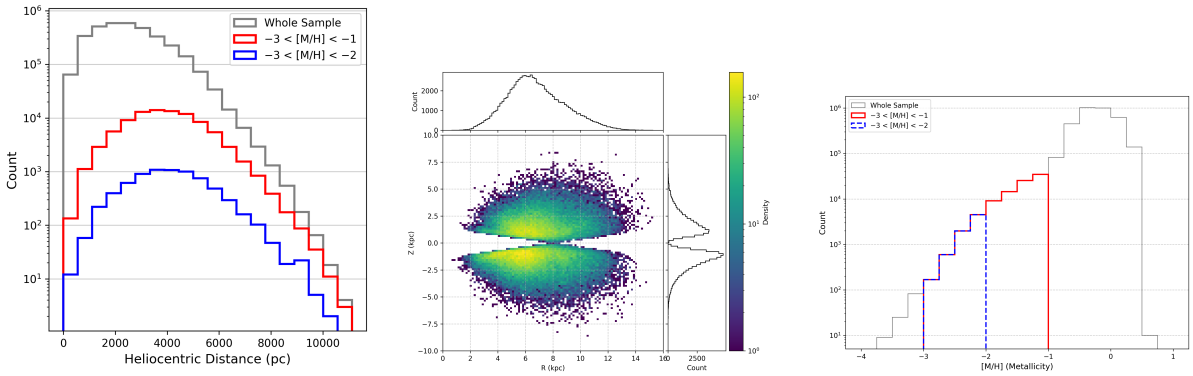

(a) Heliocentric distance (b) R–Z distribution (c) Metallicity

Figure 1: Properties of the final RGB sample after all quality and footprint cuts. *Left:* heliocentric-distance histogram for the whole sample (grey); the subsets with $-3 < [\mathrm{M/H}] < -1$ and $-3 < [\mathrm{M/H}] < -2$ are shown in solid red and dashed blue, respectively. *Middle:* density map in Galactocentric cylindrical coordinates. The empty band at low $|Z|$ is a selection artefact of our latitude/extinction cuts, which deliberately remove the thin–disc mid-plane; the concentration around $R \simeq 5$–$8\,\mathrm{kpc}$ reflects the volume accessible to bright RGB stars interior to the Solar circle and coincides with the molecular ring region where the stellar surface density peaks. *Right:* Metallicity distribution of our data sample. Line colours are the same as in the left panel.

cylindrical velocity components (v_R, v_ϕ, v_Z) are extracted from the transformed `SkyCoord` via the `CylindricalRepresentation/CylindricalDifferential` interface.

To propagate measurement errors we generate $N_{\mathrm{MC}} = 100$ Monte–Carlo realisations per star, drawing parallax, proper motions, radial velocity, and distance from their reported uncertainties (the proper–motion covariance is honoured through a bivariate normal). Each realisation is transformed to the Galactocentric frame, yielding distributions of v_R, v_ϕ, and v_Z; the 1σ widths of those distributions are stored as per–star velocity uncertainties.

As shown in Figure 2, stellar azimuthal velocities evolve strongly with metallicity. Halo–like kinematics dominate at $[\mathrm{M/H}] \lesssim -1.5\,\mathrm{dex}$: the median rotation is $|v_\phi| \lesssim 20\ \mathrm{km\ s^{-1}}$ and the 16–84 percentile span is $\sim$ 120–150 $\mathrm{km\ s^{-1}}$, indicative of a pressure-supported component. A rapid spin-up appears at $[\mathrm{M/H}] \simeq -1.3\,\mathrm{dex}$, where the median climbs to $\sim 150\ \mathrm{km\ s^{-1}}$ while the velocity spread contracts. By $[\mathrm{M/H}] \gtrsim -0.5\,\mathrm{dex}$ the median reaches the Local Standard-of-Rest value ($\approx 220\ \mathrm{km\ s^{-1}}$) and the dispersion falls below $\sim 30\ \mathrm{km\ s^{-1}}$, marking the transition to the present-day thin disc. Hence the onset of ordered rotation in the Milky Way occurred when the inter-stellar medium reached roughly one-tenth solar metallicity, and full kinematic coldness was achieved only after it became near-solar.

As illustrated in Fig. 3, stars richer than $[\mathrm{M/H}] \sim -1.0$ occupy the top of the v_R–v_ϕ plane, clustering near the thin– and thick-disc ellipses in Fig. 4. Their large prograde azimuthal velocity ($v_\phi \gtrsim 180\ \mathrm{km\ s^{-1}}$) and small radial dispersion indicate rotation-dominated, dynamically cold orbits. Below $[\mathrm{M/H}] \simeq -1.0$ the distribution broadens and drops toward $v_\phi \approx 0$, signalling a transition to pressure-supported kinematics characteristic of the stellar halo and the radial Gaia–Sausage/Enceladus debris. At the lowest metal-

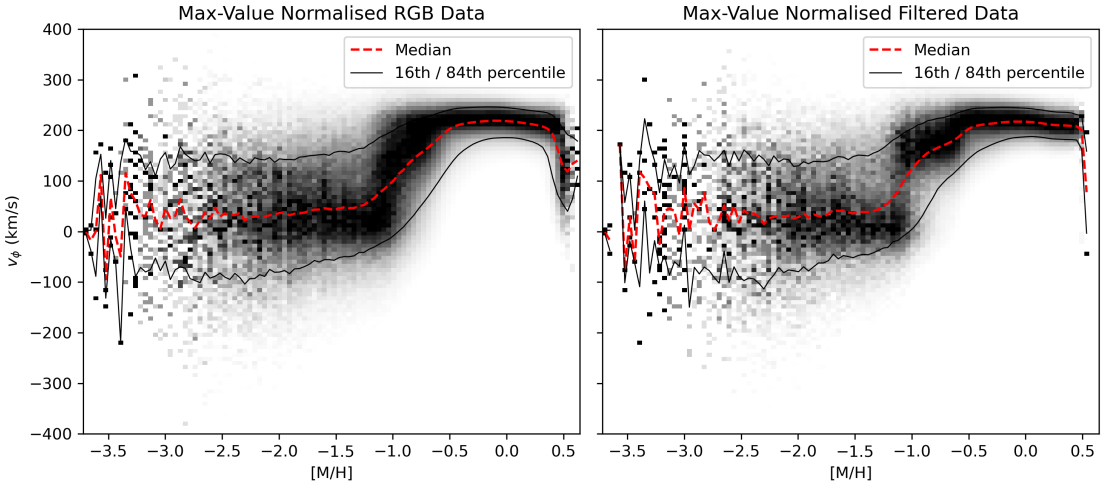

Figure 2: Column-normalised density in the v_ϕ–[M/H] plane. *Left:* the bright-RGB catalogue of Andrae et al. [2023]. *Right:* the same sample after all distance, dust, and quality cuts. Greyscale pixels show the normalised counts in each metallicity bin; the red dashed curve is the median v_ϕ, and the black curves trace the 16$^{\text{th}}$ and 84$^{\text{th}}$ percentiles.

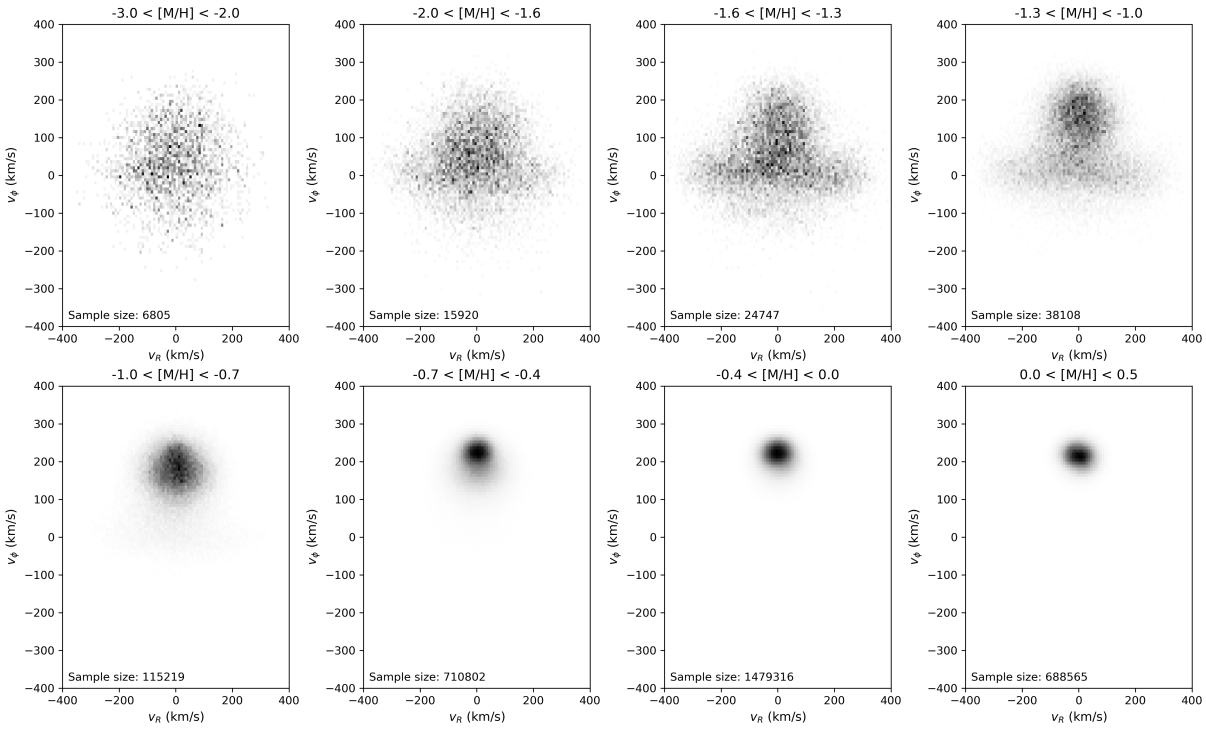

Figure 3: Galactocentric velocity distributions as a function of metallicity. Each panel shows the column–normalised density of stars in the v_R–v_ϕ plane for the metallicity interval printed at the top. With increasing metallicity the distribution contracts in both directions—signalling lower velocity dispersion—while the bulk of stars moves upward to larger prograde azimuthal velocity.

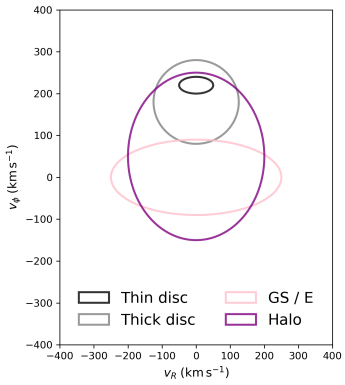

Figure 4: Ellipses mark the approximate extent of the thin disc (black), thick disc (grey), Gaia–Sausage/Enceladus debris (pink) and the pressure-supported stellar halo (purple). The figure serves as a visual key for interpreting the data panels in Fig. 3.

licities ([M/H] $\lesssim -1.5$) the contours are nearly isotropic with only a mild prograde bias, and the distinct disc sequence seen at higher metallicity has vanished. Hence, any rotation-supported very-metal-poor disc must contribute at most a small fraction of the population—an issue we quantify in following analysis

3 Methodology

Details of your methodology.

3.1 Extreme Deconvolution

Discussion of XD.

4 Results

What you found.

5 Extension direction

6 Conclusion

Summary of your findings.

References

D. An and T. C. Beers. A blueprint for the milky way's stellar populations: The power of large photometric and astrometric surveys. *The Astrophysical Journal*, 897(1):39, July 2020. doi: 10.3847/1538-4357/ab8d39. URL https://ui.adsabs.harvard.edu/abs/2020ApJ...897...39A.

F. Anders, P. Gispert, B. Ratcliffe, C. Chiappini, I. Minchev, S. Nepal, A. B. A. Queiroz, J. A. S. Amarante, T. Antoja, G. Casali, L. Casamiquela, A. Khalatyan, A. Miglio, H. Perottoni, and M. Schultheis. Spectroscopic age estimates for apogee red-giant stars: Precise spatial and kinematic trends with age in the galactic disc. *Astronomy and amp; Astrophysics*, 678:A158, Oct. 2023. ISSN 1432-0746. doi: 10.1051/0004-6361/202346666. URL http://dx.doi.org/10.1051/0004-6361/202346666.

R. Andrae, H.-W. Rix, and V. Chandra. Robust data-driven metallicities for 175 million stars from gaia xp spectra. *The Astrophysical Journal Supplement Series*, 267(1): 8, jul 2023. doi: 10.3847/1538-4365/acd53e. URL https://dx.doi.org/10.3847/1538-4365/acd53e.

A. Arentsen, E. Starkenburg, N. F. Martin, D. S. Aguado, D. B. Zucker, C. Allende Prieto, V. Hill, K. A. Venn, R. G. Carlberg, J. I. González Hernández, L. I. Mashonkina, J. F. Navarro, R. Sánchez-Janssen, M. Schultheis, G. F. Thomas, K. Youakim, G. F. Lewis, J. D. Simpson, Z. Wan, R. E. Cohen, D. Geisler, and J. E. O'Connell. The pristine inner galaxy survey (pigs) ii: Uncovering the most metal-poor populations in the inner milky way. *Monthly Notices of the Royal Astronomical Society*, 496(4): 4964–4978, July 2020a. ISSN 1365-2966. doi: 10.1093/mnras/staa1661. URL http://dx.doi.org/10.1093/mnras/staa1661.

A. Arentsen, E. Starkenburg, N. F. Martin, V. Hill, R. Ibata, A. Kunder, M. Schultheis, K. A. Venn, D. B. Zucker, D. Aguado, R. Carlberg, J. I. González Hernández, C. Lardo, N. Longeard, K. Malhan, J. F. Navarro, R. Sánchez-Janssen, F. Sestito, G. Thomas, K. Youakim, G. F. Lewis, J. D. Simpson, and Z. Wan. The pristine inner galaxy survey (pigs) i: Tracing the kinematics of metal-poor stars in the galactic bulge. *Monthly Notices of the Royal Astronomical Society*, 491(1):L11–L16, January 2020b. doi: 10.1093/mnrasl/slz156. URL https://ui.adsabs.harvard.edu/abs/2020MNRAS.491L..11A.

C. A. L. Bailer-Jones, J. Rybizki, M. Fouesneau, M. Demleitner, and R. Andrae. VizieR Online Data Catalog: Distances to 1.47 billion stars in Gaia EDR3 (Bailer-Jones+, 2021). VizieR On-line Data Catalog: I/352. Originally published in: 2021AJ....161..147B, Feb. 2021.

V. Belokurov and A. Kravtsov. From dawn till disc: Milky way's turbulent youth revealed by the apogee+gaia data. *Monthly Notices of the Royal Astronomical Society*, 514(1): 689–714, May 2022. ISSN 1365-2966. doi: 10.1093/mnras/stac1267. URL http://dx.doi.org/10.1093/mnras/stac1267.

V. Belokurov, D. Erkal, N. W. Evans, S. E. Koposov, and A. J. Deason. Co-formation of the disc and the stellar halo. *Monthly Notices of the Royal Astronomical Society*, 478(1):611–619, June 2018. ISSN 1365-2966. doi: 10.1093/mnras/sty982. URL http://dx.doi.org/10.1093/mnras/sty982.

S. A. Bird, X.-X. Xue, C. Liu, J. Shen, C. Flynn, C. Yang, G. Zhao, and H.-J. Tian. Constraints on the assembly history of the milky way's smooth, diffuse stellar halo from the metallicity-dependent, radially dominated velocity anisotropy profiles probed with k giants and bhb stars using lamost, sdss/segue, and gaia. *The Astrophysical Journal*, 919(1):66, Sept. 2021. ISSN 1538-4357. doi: 10.3847/1538-4357/abfa9e. URL http://dx.doi.org/10.3847/1538-4357/abfa9e.

J. Bland-Hawthorn and O. Gerhard. The galaxy in context: Structural, kinematic, and integrated properties. *Annual Review of Astronomy and Astrophysics*, 54(1):529–596, Sept. 2016. ISSN 1545-4282. doi: 10.1146/annurev-astro-081915-023441. URL http://dx.doi.org/10.1146/annurev-astro-081915-023441.

J. S. Bullock and M. Boylan-Kolchin. Small-scale challenges to the lambda cdm paradigm. *Annual Review of Astronomy and Astrophysics*, 55(1):343–387, Aug. 2017. ISSN 1545-4282. doi: 10.1146/annurev-astro-091916-055313. URL http://dx.doi.org/10.1146/annurev-astro-091916-055313.

D. Carollo, M. Chiba, M. Ishigaki, K. Freeman, T. C. Beers, Y. S. Lee, P. Tissera, C. Battistini, and F. Primas. Evidence for the third stellar population in the milky way's disk. *The Astrophysical Journal*, 887(1):22, December 2019. doi: 10.3847/1538-4357/ab517c. URL https://ui.adsabs.harvard.edu/abs/2019ApJ...887...22C.

M. Chiba and T. C. Beers. Kinematics of metal-poor stars in the galaxy. iii. formation of the stellar halo and thick disk as revealed from a large sample of nonkinematically selected stars. *The Astronomical Journal*, 119(6):2843–2865, June 2000. ISSN 0004-6256. doi: 10.1086/301409. URL http://dx.doi.org/10.1086/301409.

A. P. Cooper, S. Cole, C. S. Frenk, S. D. M. White, J. Helly, A. J. Benson, G. De Lucia, A. Helmi, A. Jenkins, J. F. Navarro, V. Springel, and J. Wang. Galactic stellar haloes in the cdm model: Galactic stellar haloes in the cdm model. *Monthly Notices of the Royal Astronomical Society*, 406(2):744–766, May 2010. ISSN 0035-8711. doi: 10.1111/j.1365-2966.2010.16740.x. URL http://dx.doi.org/10.1111/j.1365-2966.2010.16740.x.

G. Cordoni, G. S. Da Costa, D. Yong, A. D. Mackey, A. F. Marino, S. Monty, T. Nordlander, J. E. Norris, M. Asplund, M. S. Bessell, A. R. Casey, A. Frebel, K. Lind, S. J. Murphy, B. P. Schmidt, X. D. Gao, T. Xylakis-Dornbusch, A. M. Amarsi, and A. P. Milone. Exploring the galaxy's halo and very metal-weak thick disc with skymapper and gaia dr2. *Monthly Notices of the Royal Astronomical Society*, 503 (2):2539–2561, Nov. 2020. ISSN 1365-2966. doi: 10.1093/mnras/staa3417. URL http://dx.doi.org/10.1093/mnras/staa3417.

A. M. Dillamore, V. Belokurov, N. W. Evans, and E. Y. Davies. Stellar halo substructure generated by bar resonances. *Monthly Notices of the Royal Astronomical Society*, 524 (3):3596–3608, July 2023. ISSN 1365-2966. doi: 10.1093/mnras/stad2136. URL http://dx.doi.org/10.1093/mnras/stad2136.

S. M. Fall and R. Chandar. Similarities in populations of star clusters. *The Astrophysical Journal*, 752(2):96, may 2012. doi: 10.1088/0004-637X/752/2/96. URL https://dx.doi.org/10.1088/0004-637X/752/2/96.

Gaia Collaboration, A. Vallenari, A. G. A. Brown, et al. Gaia data release 3: Summary

of the content and survey properties. *Astronomy & Astrophysics*, 674:A1, 2023. doi: 10.1051/0004-6361/202243940.

G. M. Green. dustmaps: A python interface for maps of interstellar dust. *Journal of Open Source Software*, 3(26):695, 2018. doi: 10.21105/joss.00695. URL https://doi.org/10.21105/joss.00695.

A. B. Gurvich, J. Stern, C.-A. Faucher-Giguère, P. F. Hopkins, A. Wetzel, J. Moreno, C. C. Hayward, A. J. Richings, and Z. Hafen. Rapid disc settling and the transition from bursty to steady star formation in milky way-mass galaxies. *Monthly Notices of the Royal Astronomical Society*, 519(2):2598–2614, February 2023. doi: 10.1093/mnras/stac3712. URL https://ui.adsabs.harvard.edu/abs/2023MNRAS.519.2598G.

M. Haywood, P. Di Matteo, M. D. Lehnert, D. Katz, and A. Gómez. The age structure of stellar populations in the solar vicinity: Clues of a two-phase formation history of the milky way disk. *Astronomy and amp; Astrophysics*, 560:A109, Dec. 2013. ISSN 1432-0746. doi: 10.1051/0004-6361/201321397. URL http://dx.doi.org/10.1051/0004-6361/201321397.

A. Helmi. Streams, substructures, and the early history of the milky way. *Annual Review of Astronomy and Astrophysics*, 58(1):205–256, Aug. 2020. ISSN 1545-4282. doi: 10.1146/annurev-astro-032620-021917. URL http://dx.doi.org/10.1146/annurev-astro-032620-021917.

A. Helmi and P. Tim de Zeeuw. Mapping the substructure in the galactic halo with the next generation of astrometric satellites. *Monthly Notices of the Royal Astronomical Society*, 319(3):657–665, 2000.

A. Helmi, C. Babusiaux, H. H. Koppelman, D. Massari, J. Veljanoski, and A. G. A. Brown. The merger that led to the formation of the milky way's inner stellar halo and thick disk. *Nature*, 563(7729):85–88, Oct. 2018. ISSN 1476-4687. doi: 10.1038/s41586-018-0625-x. URL http://dx.doi.org/10.1038/s41586-018-0625-x.

L. Lancaster, S. E. Koposov, V. Belokurov, N. W. Evans, and A. J. Deason. The halo's ancient metal-rich progenitor revealed with bhb stars. *Monthly Notices of the Royal Astronomical Society*, 486(1):378–389, Mar. 2019. ISSN 1365-2966. doi: 10.1093/mnras/stz853. URL http://dx.doi.org/10.1093/mnras/stz853.

H. W. Leung and J. Bovy. Deep learning of multi-element abundances from high-resolution spectroscopic data. *Monthly Notices of the Royal Astronomical Society*, 483 (3):3255–3277, 2019.

M. K. Mardini, A. Frebel, A. Chiti, Y. Meiron, K. V. Brauer, and X. Ou. The atari disk, a metal-poor stellar population in the disk system of the milky way. *The Astrophysical Journal*, 936(1):78, Sept. 2022. ISSN 1538-4357. doi: 10.3847/1538-4357/ac8102. URL http://dx.doi.org/10.3847/1538-4357/ac8102.

P. J. McMillan. The mass distribution and gravitational potential of the milky way. *Monthly Notices of the Royal Astronomical Society*, 465(1):76–94, Oct. 2016. ISSN 1365-2966. doi: 10.1093/mnras/stw2759. URL http://dx.doi.org/10.1093/mnras/stw2759.

B. Nordström, M. Mayor, J. Andersen, J. Holmberg, F. Pont, B. R. Jørgensen, E. H.

Olsen, S. Udry, and N. Mowlavi. The geneva-copenhagen survey of the solar neighbourhood: Ages, metallicities, and kinematic properties of ∼14 000 f and g dwarfs. *Astronomy and amp; Astrophysics*, 418(3):989–1019, Apr. 2004. ISSN 1432-0746. doi: 10.1051/0004-6361:20035959. URL http://dx.doi.org/10.1051/0004-6361:20035959.

J. Norris, M. S. Bessell, and A. J. Pickles. Population studies. i. the bidelman-macconnell "weak-metal" stars. *The Astrophysical Journal Supplement Series*, 58:463–492, July 1985. doi: 10.1086/191049. URL https://ui.adsabs.harvard.edu/abs/1985ApJS..58..463N.

A. B. Pace. The Local Volume Database: a library of the observed properties of nearby dwarf galaxies and star clusters. *arXiv e-prints*, art. arXiv:2411.07424, Nov. 2024. doi: 10.48550/arXiv.2411.07424.

C. W. Purcell, J. S. Bullock, and A. R. Zentner. Shredded galaxies as the source of diffuse intrahalo light on varying scales. *The Astrophysical Journal*, 666(1):20–33, Sept. 2007. ISSN 1538-4357. doi: 10.1086/519787. URL http://dx.doi.org/10.1086/519787.

H.-W. Rix, V. Chandra, R. Andrae, A. M. Price-Whelan, D. H. Weinberg, C. Conroy, M. Fouesneau, D. W. Hogg, F. De Angeli, R. P. Naidu, M. Xiang, and D. Ruz-Mieres. The poor old heart of the milky way. *The Astrophysical Journal*, 941(1):45, Dec. 2022. ISSN 1538-4357. doi: 10.3847/1538-4357/ac9e01. URL http://dx.doi.org/10.3847/1538-4357/ac9e01.

I. B. Santistevan, A. Wetzel, R. E. Sanderson, K. El-Badry, J. Samuel, and C.-A. Faucher-Giguère. The origin of metal-poor stars on prograde disc orbits in fire simulations of milky way-mass galaxies. *Monthly Notices of the Royal Astronomical Society*, 505 (1):921–938, July 2021. doi: 10.1093/mnras/stab1345. URL https://ui.adsabs.harvard.edu/abs/2021MNRAS.505..921S.

R. Schönrich, J. Binney, and W. Dehnen. Local kinematics and the local standard of rest. *Monthly Notices of the Royal Astronomical Society*, 403(4):1829–1833, Apr. 2010. ISSN 1365-2966. doi: 10.1111/j.1365-2966.2010.16253.x. URL http://dx.doi.org/10.1111/j.1365-2966.2010.16253.x.

F. Sestito, N. Martin, and E. Starkenburg. Tracing the formation of the milky way through ultra metal-poor stars. In *The Gaia Universe*, page 47, Apr. 2019. doi: 10.5281/zenodo.3236051.

F. Sestito, T. Buck, E. Starkenburg, N. F. Martin, J. F. Navarro, K. A. Venn, A. Obreja, P. Jablonka, and A. V. Macciò. Exploring the origin of low-metallicity stars in milky-way-like galaxies with the nihao-uhd simulations. *Monthly Notices of the Royal Astronomical Society*, 500(3):3750–3762, Nov. 2020. ISSN 1365-2966. doi: 10.1093/mnras/staa3479. URL http://dx.doi.org/10.1093/mnras/staa3479.

K. A. Venn, C. L. Kielty, F. Sestito, E. Starkenburg, N. Martin, D. S. Aguado, A. Arentsen, P. Bonifacio, E. Caffau, V. Hill, P. Jablonka, C. Lardo, L. Mashonkina, J. F. Navarro, C. Sneden, G. Thomas, K. Youakim, J. I. González-Hernández, R. S. Janssen, R. Carlberg, and K. Malhan. The pristine survey - ix. cfht espadons spectroscopic analysis of 115 bright metal-poor candidate stars. *Monthly Notices of the Royal Astronomical Society*, 492(3):3241–3262, Mar. 2020. doi: 10.1093/mnras/stz3546.

H. Zhang, A. Ardern-Arentsen, and V. Belokurov. On the existence of a very metal-poor disc in the milky way, 2024. URL https://arxiv.org/abs/2311.09294.